Effect of thermal treatment on the synthesis of $NiAl_2O_4$ spinel oxide using chitosan as precursor

(Efeito do tratamento térmico na síntese do óxido espinélio $NiAl_2O_4$ usando quitosana como precursor)

C. G. Anchieta[1], L. Tochetto[1], H. B. Madalosso[1], R. D. Sulkovski[1], C. Serpa[1], M. A. Mazutti[1], A. R. F. de Almeida[2], A. Gündel[2], E. L. Foletto[1]*

[1]Department of Chemical Engineering, Federal University of Santa Maria, 97105-900, Santa Maria, RS, Brazil
[2]University Campus, Federal University of Pampa, 96413-170, Bagé, RS, Brazil
**efoletto@gmail.com*

Abstract

Nickel aluminate oxide ($NiAl_2O_4$) was prepared using chitosan as polymeric precursor and ammonia solution as a precipitating agent. In addition, nickel nitrate and aluminum nitrate salts were used as sources of Ni and Al, under stoichiometric amounts (molar ratio Ni:Al = 1:2). $NiAl_2O_4$ particles were prepared at different calcination temperatures and their properties were investigated. The synthesized materials were characterized by X-ray diffraction, infrared spectroscopy, atomic force microscopy, thermogravimetric analysis and nitrogen adsorption-desorption isotherms. The results showed that the thermal treatment process strongly influence on the formation of a single-phase structure of $NiAl_2O_4$ spinel. Nickel aluminate spinel with a porous structure and high surface area was obtained at temperatures above 700 °C.
Keywords: nickel aluminate, synthesis, characterization, chitosan, porous material.

Resumo

Aluminato de níquel ($NiAl_2O_4$) foi preparado utilizando quitosana como precursor polimérico e uma solução amoniacal como um agente de precipitação. Além disso, sais de nitrato de níquel e de nitrato alumínio foram empregados como fontes de Ni e Al, em quantidades estequiométricas (razão molar Ni:Al = 1:2). Partículas de $NiAl_2O_4$ foram preparadas em diferentes temperaturas de calcinação e as suas propriedades foram investigadas. Os sólidos sintetizados foram caracterizados por difração de raios X, espectroscopia de infravermelho, microscopia de força atômica, análise termogravimétrica e isotermas de adsorção-dessorção de nitrogênio. Os resultados mostraram que o processo de tratamento térmico influencia fortemente sobre formação da fase espinélio $NiAl_2O_4$. Partículas de aluminato de níquel, com uma estrutura porosa e com alta área superficial, foram obtidas em temperaturas superiores a 700 °C.
***Palavras-chave**: aluminato de níquel, síntese,caracterização, quitosana, material poroso .*

INTRODUCTION

Nickel aluminate ($NiAl_2O_4$) is a ternary oxide with AB_2O_4 spinel structure, where A and B are cations occupying tetrahedral (Ni^{2+}) and octahedral (Al^{3+}) sites, respectively [1]. Due to its high mechanical resistance, as well as its high thermal and chemical stabilities, nickel aluminate has been employed as catalyst support in various chemical reactions such as 1, 2, 4-trichlorobenzene hydrodechlorination [2], partial oxidation of methane to syngas [3], CO_2 reforming of methane [4], chemical-looping combustion [5, 6], acetylene hydrogenation [7], steam reforming of methane [8, 9], combustion of methane [10] and steam reforming of glycerol to hydrogen production [11]. $NiAl_2O_4$ particles have been prepared by various routes such as sol-gel [12, 13], solid state reaction [14], microwave [15, 16], sonochemical [17], Pechini method [18], thermal decomposition of polynuclear malate complexes [19], mechano-chemical synthesis [20], one-pot process [21] and combustion route [22-24]. In this work, we proposethe use of an alternative route for the preparation of $NiAl_2O_4$ spinel. In this alternative route the combustion of chitosan precursor results in the generation of a material with porous structure and high surface area [25], which are very important properties for catalytic and adsorptive purposes. Although some materials such as the binary oxides magnesia [26], ceria [27], silica [28], and alumina [29] and ternary oxides magnesium aluminate [30] and zinc aluminate [31, 32] have been synthesized by this route, the preparation of nickel aluminate oxide ($NiAl_2O_4$) has not been yet investigated.

In this context, the objective of this work was to investigate the influence of the thermal treatment on thephysical characteristics of nickel aluminate oxide obtained by use of chitosan as precursor. The synthesized

samples were characterized by different techniques and so their physical properties were determined.

MATERIALS AND METHODS

$NiAl_2O_4$ particles were prepared from aluminum nitrate (analytical grade), nickel nitrate (analytical grade) and chitosan polymer [$(C_6H_{11}O_4N)_n$] (Purifarma, Brazil). All the chemicals were used as received. Synthesis procedure was carried out based on a previous work [25]. In this procedure, stoichiometric amounts of Ni and Al nitrates (molar ratio Ni:Al = 1:2) were used for the synthesis. Typically, 0.45 g of chitosanwere dissolved in 30 mL acetic acid aqueous solution (5% v/v) (solution A), 2.25 g of aluminum nitrate were dissolved in 5 mL distilled water (solution B) and, 0.87 g of nickel nitrate were dissolvedin 2 mL distilled water (solution C). After, the B and C solutions were added to solution A, under magnetic stirring for 30 min. The resulting solution was slowly added in 100 mL ammonia aqueous solution (50 %, v/v), under magnetic stirring. The particles formed were then separated from the solution and further dried at ambient temperature for 72 h. This material was then treated in an oxidizing atmosphere (air) at temperatures of 500 °C to 800 °C, for 4 h to get the $NiAl_2O_4$ particles. A conventional furnace was used for the thermal treatment process, at a heating rate of 5 °Cmin^{-1} up to the desired temperature.

X-ray diffraction (XRD) patterns of the samples were obtained with a Rigaku Miniflex300 diffractometer, in a scan 2θ range between 20° and 70°, with a step size of 2θ = 0.03° and a counting time of 0.9 s per step, with Cukα radiation (λ = 1.5418 Å) and operating at 30 kV and 10 mA. Phase identification was done by comparison with JCPDS data base file (10-0339). The average crystallite size of the samples was determined with the Scherrer equation [33]: $D = K\lambda/(h_{1/2}.\cos\theta)$, where D is the average crystallite size, K the Scherrer constant (0.9), λ the wavelength of incident X-ray (0.15418 nm), $h_{1/2}$ the width at half height of themost intense diffraction peak and θ corresponds to the peak position (in this work, 2θ= 37.01°). Fourier Transform Infrared (FTIR) spectra of samples were recorded with Shimadzu IRPrestige-21spectrophotometer in the range 4000-400 cm^{-1}, using KBr pellets (10 mg $NiAl_2O_4$/300 mg KBr). Nitrogen adsorption/desorption isotherms were obtained with an ASAP 2020 apparatus. Before analysis, the samples were degassed at 200 °C under vacuum inside the apparatus.The isotherms were measured at liquid nitrogen temperature (77 K), and nitrogen pressures ranging from 0.1 to 0.98 P/Po. Specific surface areas were calculated according to the Brunauer-Emmett-Teller (BET) method, and the pore size distributions were obtained accordingto the Barret-Joyner-Halenda (BJH) method [34] from the adsorption data. The image of particles was obtained by atomic force microscopy (AFM) (Agilent Technologies 5500). AFM images were acquired at room temperature, in non-contact mode using high resolution probes SSS-NCL (Nanosensors, force constant = 48 Nm^{-1}, resonance frequency = 154 kHz). AFM images were analyzed using scanning probe microscopy data analysis software (Gwyddion). Thermogravimetric analysis (TGA) was carried out on TGA-50 Shimadzu analyzer at a heating rate of 10 °C min^{-1} under air flow rate of 50 mL/min. For all characterization analyses, except AFM, the particles were comminuted to pass in 200 mesh sieve, before each analysis.

RESULTS AND DISCUSSION

X-ray powder diffraction patterns for all samples thermally treated above 500 °C during 4 h are shown in Fig. 1. Only for the samples treated at 500 °C and 600 °C there is not formation of a single-phase $NiAl_2O_4$ spinel structure. Thus $NiAl_2O_4$ spinel structure was only obtained when the precursor was treated above 700 °C. For the samples heated at 700 °C and 800 °C, the characteristic peaks of spinel phase can be observed. The main diffraction peaks are in agreement with the JCPDS (10-0339) data of the face-centered cubic structure of $NiAl_2O_4$spinel. The peaks at 2θ values of 31.40°, 37.01°, 44.99°, 55.98°, 59.66° and 65.53° correspond to (220), (311), (400), (422), (511) and (440) diffraction planes of the $NiAl_2O_4$spinel, respectively. The average crystallite size was calculated from Scherrer equation for $NiAl_2O_4$ samples heated at 700 and 800 °C, and

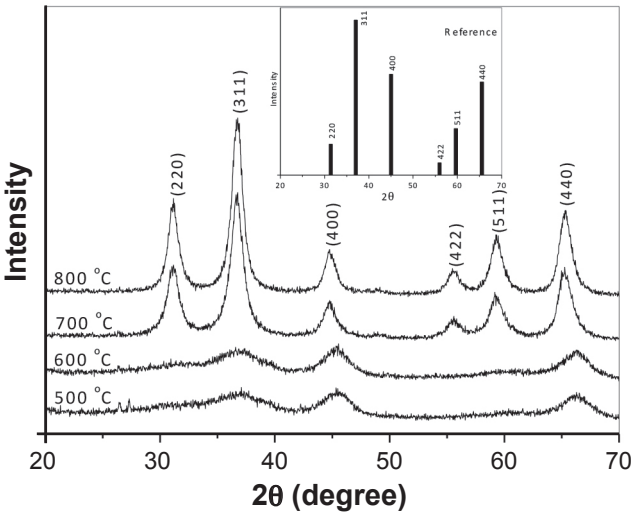

Figure 1: X-ray diffraction patterns of samples treated at different calcination temperatures. (The inset in Fig. 1 shows a reference JCPDS 10-0339).

[Figura 1: Difratogramas de raios X das amostras tratadas a diferentes temperaturas de calcinação. (Fig. interna mostra o padrão conforme arquivo JCPDS 10-0339) .]

it was 8.50 and 9.95 nm, respectively.

Fig. 2 shows the FTIR spectra of samples prepared at different calcination temperatures. FTIR spectra of samples heated at 700 °C and 800 °C s how characteristic vibrational peaks of the spinel phase in the range 500-900 cm^{-1}, which are associated with the vibrations of metal-O, Al-O, and metal-O-Al bonds [35]. The samples prepared at 500 °C and 600 °C do not present peaks in this range. This indicates that there was no formation of single-phasespinelin these

temperatures, corroborating the results of X-ray diffraction analysis. The Al-O stretching bands obs erved in the range 500-900 cm^{-1} can be assigned to different coordination states of Al atoms (AlO_6 and AlO_4). The stretching frequency found around 550 cm^{-1} can be assigned to the vibration of Ni-O bond. The broad peak at 3450 cm^{-1} is assigned to surface adsorbed water. The band at 1630 $cm^{-1}$is probably

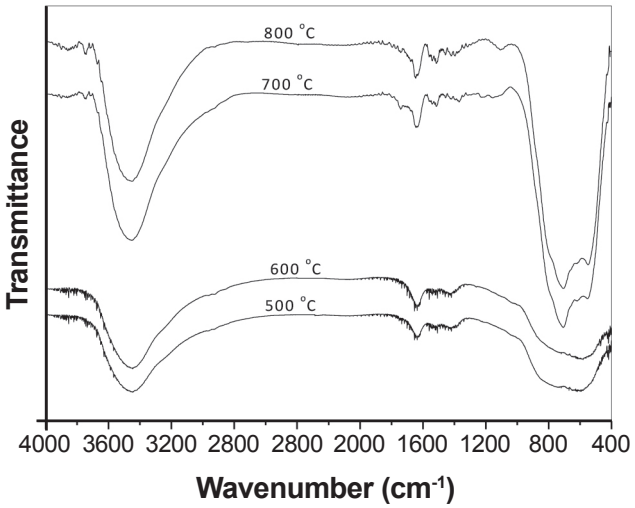

Figure 2: FTIR spectra of samples prepared at different calcination temperatures.
[Figura 2: Espectros de infravermelho das amostras preparadas em diferentes temperaturas de calcinação.]

due to the deformation vibrations of water molecules [35].

Fig. 3 shows the nitrogen adsorption–desorption isotherms and pore size distribution curves of $NiAl_2O_4$ samples formed at 700 °C and 800 °C. The shapes of the isotherms shown in Fig. 3a were similar for the two samples, showing a hysteresis loop at a high relative pressure, which can be classified astype IV according to IUPAC classification [36], indicating presence of predominantly mesoporous materials. The corresponding pore size distribution curves were obtained according to the Barrett-Joyner-Halenda (BJH) method, which are shown in Fig. 3b. Both $NiAl_2O_4$ samples display a similar unimodal distribution with peaks centered in the mesoporous region (between 20 and 500 Å). The total pore volumes for $NiAl_2O_4$ samples heated at 700 °C and 800 °C are 0.384 and 0.352 cm^3/g, respectively, whereas the average pore sizes are 88.5 Å and 94.3Å, respectively. In addition, both samples present high surface area, with strong reduction of surface area for the heated sample at 800 °C (126 m^2/g) in comparison with the heated sample at 700 °C (154m^2/g), indicating that the increase of heating temperature causes a decrease of them. For purposes of comparison, some values of surface area can be found in literature for $NiAl_2O_4$ powders synthesized by other methods, such as 22-35 m^2/g (combustion reaction using glycine as fuel) [23], 42.3 m^2/g (mechanochemical synthesis) [20], 107 m^2/g (microwave combustion) [35], 108 m^2/g (sonochemical) [17], 58-119 m^2/g (sol-gel using gelatin as organic precursor) [37], 138 m^2/g (sol-gel using propionic acid as solvent) [4], 186 m^2/g

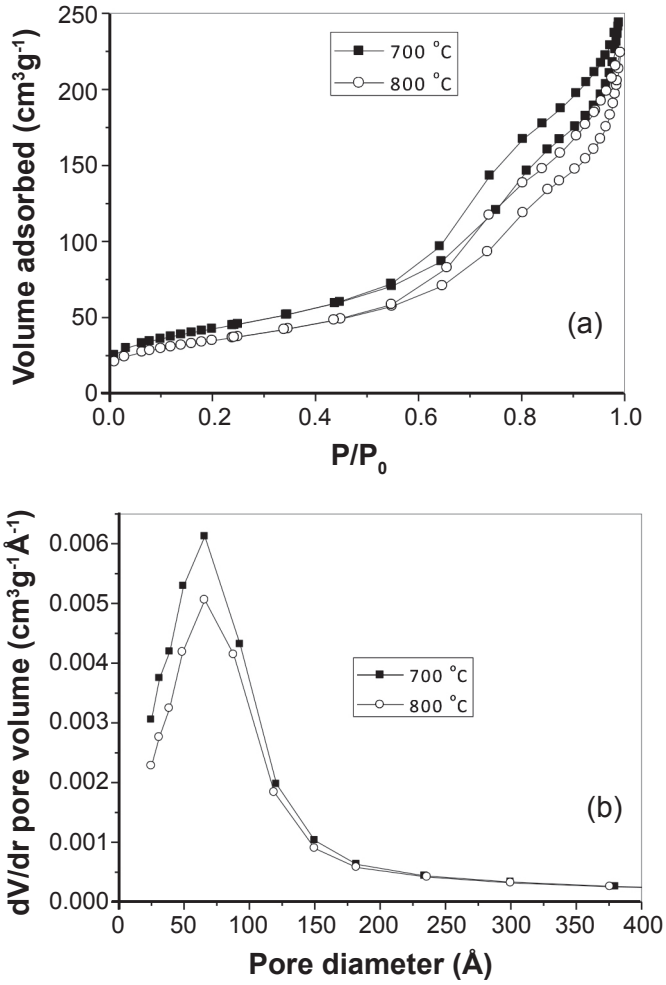

Figure 3: N_2 adsorption/desorption isotherms (a), and pore size distribution curves (b) for the $NiAl_2O_4$ samples prepared at 700 °C and 800 °C.
[Figura 3: Isotermas de adsorção/dessorção de N_2(a), distribuições do tamanho de poros (b) para as amostras de $NiAl_2O_4$ preparadas a 700 °C e 800 °C.]

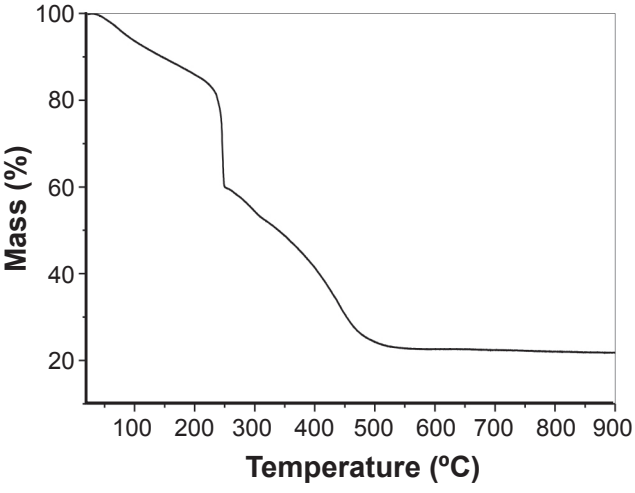

Figure 4: TGA curve of the precursor particle (before calcination).
[Figura 4: Curva ATG do material precursor (antes da calcinação).]

(combustion reaction using urea as fuel) [22], and 200-300 m^2/g (sol-gel using metal alkoxide precursors) [12]. Despite sol-gel method using metal alkoxide precursors [12] and combustion route using urea as fuel [22] generate powders with higher surface area, the method proposed in this workalso resulted intoa material containing a high surface area, comparable and superior than the ones obtained by other routes. Besides obtaining a material with high surface area, the synthesis route proposed in this work is easier and simpler because it does not need sophisticated procedures and requires inexpensive precursors.

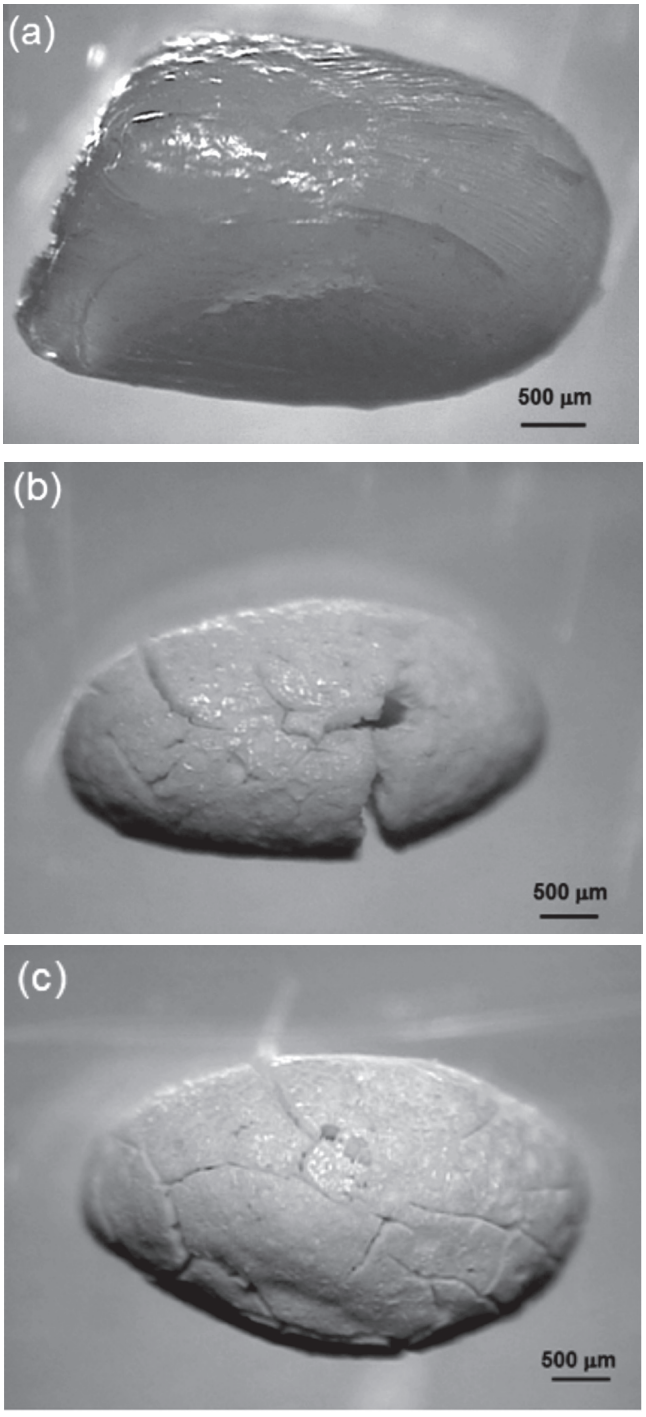

Figure 5: Images of the particles before (a), and after the thermal process at 700 °C (b) and 800 °C (c).
[Figura 5: Imagens das partículas antes (a) e após o processo térmico a 700 °C (b) e 800 °C (c).]

Fig. 4 shows the thermogravimetric analysis of precursor material (before calcination). As it can be observed, two mass loss stages occur; first, in the temperature range 25-250 °C, attributed to the elimination of physically adsorbed molecular water and decomposition of nitrates, and second, between 250 and 500 °C, related to the decomposition of chitosan. However, no further weight loss was observed above 500 °C.

Fig. 5 shows the morphology of a (a) precursor particle (before calcination) and $NiAl_2O_4$ particles prepared at (b) 600 and (c) 800 °C, as measured by atomic force microscopy (AFM). The average size of precursor particle was around 3 mm. After calcination process, the particles presented a smaller size due to the elimination of water, nitrates and chitosan, as mentioned in the termogravimetric analysis (see Fig. 4). Furthermore, the particles presented crack on its structure, and this occurs mainly due to the burning of organic matter (chitosan), which causes the formation of pores as the volatile substances are eliminated [38]. This leads to the formation of a porous structure and an increase in the surface area, which are desirable characteristics for catalytic and adsorptive purposes.

CONCLUSIONS

The technique using chitosan as template was very promising for the production of nickel aluminate oxide. Chitosan plays a very important role on the synthesis: production of solid materials with mesoporous structure. From characterization techniques, it is possible to observe that the single-phase structure of $NiAl_2O_4$ spinel was only formed when the precursor particles were treated at temperatures above 700 °C. The synthesized material shows a predominantly mesoporous structure and with high surface area (154 m^2/g). Therefore, this method has a great advantage that consists in the production of porous $NiAl_2O_4$ oxide for application in the field of catalysis and adsorption. In summary, this route is easy, simple and environmental friendly (surfactant free), and it can be applied as an alternative route to produce other spinel powders.

ACKNOWLEDGEMENTS

The authors would like to thank the agencies FAPERGS and CNPq for their financial support.

REFERENCES

[1] Y.S. Han, J.B. Li, X.S. Ning, X.Z. Yang, B. Chi, Mat. Sci. Eng. A **369** (2004) 241.
[2] Y. Cesteros, P. Salagre, F. Medina, J.E. Sueiras,Studies Surf. Sci. Catal. **130** (2000) 2069.
[3] R. López-Fonseca, C. Jiménez-González, B. Rivas, J.I. Gutiérrez-Ortiz, Appl. Catal. A: Gen. **437-438** (2012) 53.

[4] N. Sahli, C. Petit, A.C. Roger, A. Kiennemann, S. Libs, M. M. Bettahar, Catal. Today **113** (2006) 187.
[5] H. Jin, T. Okamoto, M. Ishida, J. Ind. Eng. Chem. Res. **38** (1999) 126.
[6] H. Zhao, L. Liu, D. Xu, C. Zheng, G. Liu, L. Jiang, J. Fuel Chem. Technol. **36** (2008) 261.
[7] J.A. Peña, J.C. Rodríguez, J. Herguido, J. Santamaría, A. Monzón, Studies Surf. Sci. Catal. **88** (1994) 555.
[8] L. Zhou, Y. Guo, Q. Zhang, M. Yagi, J. Hatakeyama, H. Li, J. Chen, M. Sakurai, H. Kameyama, Appl.Catal. A: Gen. **347** (2008) 200.
[9] T. Numaguchi, H. Eida, K. Shoji, Int. J. Hydrogen Energy **22** (1997) 1111.
[10] M.M. Yazdanpanah, A. Forret, T. Gauthier, A. Delebarre, Appl. Energy **113** (2014)1933.
[11] B. Dou, C. Wang, H. Chen, Y. Song, B. Xie, Int. J. Hydrogen Energy **38** (2013) 11902.
[12] C.O. Areán, M. P. Mentruit, A.J.L. López, J.B. Parra, Coll. Surf. A: Physicochem. Eng. Aspects **180** (2001) 253.
[13] N. Bayal, P. Jeevanandam, J. Alloys Compds. **516** (2012) 27.
[14] C.Y. Li, H.J. Zhang, Z.Q. Chen,Appl. Surf. Sci. **266** (2013) 17.
[15] M.M. Amini, L. Torkian, Mater. Lett. **57** (2002) 639.
[16] R.D. Peelamedu, R. Roy, D. K. Agrawal, Mater. Lett. **55** (2002)234.
[17] P. Jeevanandam, Y. Koltypin, A. Gedanken, Mater. Sci. Eng. B **90** (2002) 125.
[18] L. Gama, M.A. Ribeiro, B.S. Barros, R.H.A. Kiminami, I. T. Weber, A.C.F.M. Costa, J. Alloys Compds. **483** (2009) 453.
[19] C. Suciu, L. Patron, I. Mîndru, O. Carp, Rev. Roumaine Chimie **51** (2006) 385.
[20] M.K. Nazemi, S. Sheibani, F. Rashchi, V.M.G.D. Cruz, A. Caballero, Adv. Powder Technol. **23** (2012) 833.
[21] P. Hasin, N. Koonsaeng, A. Laobuthee, Mj. Int. J. Sci. Technol. **2** (2008) 140.
[22] N.F.P. Ribeiro, R.C.R. Neto, S.F. Moya, M.M.V.M. Souza, M. Schmal, Int. J. Hydrogen Energy **35** (2010) 11725.
[23] E. Leal, A.C.F.M. Costa, N.L. Freita, H.L. Lira, R. H.G.A. Kiminami, L. Gama, Mater. Res. Bull. **46** (2011) 1409.
[24] N.M. Deraz, Int. J. Electrochem. Sci. **8** (2013) 5203.
[25] G.D. B. Nuernberg, E.L. Foletto, L.F.D. Probst, C.E. M. Campos, N.L.V. Carreño, M.A. Moreira, Chem. Eng. J. **193-194** (2012) 211.
[26] G.I. Almerindo, L.F.D. Probst, C.E.M. Campos, R.M. Almeida, S.M.P. Meneghetti, M.R. Meneghetti, J. Clacens, H. V. Fajardo, J. Power Sources **196** (2011) 8057.
[27] A.B. Sifontes, G. Gonzalez, J.L. Ochoa, L. M. Tovar, T. Zoltan, E. Cañizales, Mater. Res. Bull. **46** (2011) 1794.
[28] T.P. Braga, E.C.C. Gomes, A.F. Sousa, N.L.V. Carreño, E. Longhinotti, A. Valentini, J. Non-Cryst.Solids **355** (2009) 860.
[29] R.M. Almeida, H.V. Fajardo, D.Z. Mezalira, G.B. Nuernberg, L.K. Noda, L.F.D. Probst, N.L.V. Carreño, J. Mol. Catal. A: Chem. **259** (2006) 328.
[30] G.D.B. Nuernberg, E.L. Foletto, L.F.D. Probst, N.L.V. Carreño, M.A. Moreira, J. Mol.Catal. A: Chem. **370** (2013) 22.
[31] C.G. Anchieta, D. Sallet, E.L. Foletto, S.S. Silva, O. Chiavone-Filho, C.A.O. Nascimento, Ceram. Int. **40** (2014) 4173.
[32] F.M. Stringhini, E.L. Foletto, D. Sallet, D.A. Bertuol, O. Chiavone-Filho, C.A.O. Nascimento, J. Alloys Compds. **588** (2014) 305.
[33] B.D. Cullity, S. R. Stock, *Elements of X-ray diffraction*, 3rd Ed., Prentice-Hall Inc., New Jersey, USA (2001).
[34] E. P. Barret, L. G. Joyner, P. P. Halenda, J. Am. Chem. Soc. **73** (1951) 373.
[35] C. Ragupathi, J. J. Vijaya, L. J. Kennedy, "Preparation, characterization and catalytic properties of nickel aluminate nanoparticles: A comparison between conventional and microwave method", J. Saudi Chem. Soc., in press, DOI: http://dx.doi.org/10.1016/j.jscs.2014.01.006.
[36] Int. Union Pure Appl. Chem.(IUPAC) **57** (1985) 603.
[37] N.A.S. Nogueira, E.B. Silva, P.M. Jardim, J.M. Sasaki, Mater. Letters **61** (2007) 4743.
[38] T. P. Braga, E. Longhinotti, A.N. Pinheiro, A. Valentini, J. Appl. Catal. A: Gen. **362** (2009) 139.
(Rec. 15/04/2015, Rev. 08/07/2015, Ac. 27/08/2015)